frontiers | Frontiers in Marine Science

TYPE Original Research
PUBLISHED 08 September 2022
DOI 10.3389/fmars.2022.934391

OPEN ACCESS

EDITED BY
Fajin Chen,
Guangdong Ocean University, China

REVIEWED BY
Tarron Lamont,
Department of Environment, Forestry and Fisheries (DEFF), South Africa
Haibin Lü,
Jiangsu Ocean University, China

*CORRESPONDENCE
Yuyuan Xie
xieyuyuan@hotmail.com
Bangqin Huang
bqhuang@xmu.edu.cn

SPECIALTY SECTION
This article was submitted to Marine Biogeochemistry, a section of the journal Frontiers in Marine Science

RECEIVED 02 May 2022
ACCEPTED 16 August 2022
PUBLISHED 08 September 2022

CITATION
Liu H, Xie Y, Browning TJ, Xu F and Huang B (2022) Phytoplankton photophysiology across tropical eddies: Deconvolving nutrient, light, and community signals. *Front. Mar. Sci.* 9:934391. doi: 10.3389/fmars.2022.934391

Phytoplankton photophysiology across tropical eddies: Deconvolving nutrient, light, and community signals

Haoran Liu[1,2], Yuyuan Xie[1,3]*, Thomas J. Browning[2], Feipeng Xu[1] and Bangqin Huang[1]*

[1]State Key Laboratory of Marine Environmental Science, Fujian Provincial Key Laboratory of Coastal Ecology and Environmental Studies, Xiamen University, Xiamen, China, [2]Marine Biogeochemistry Division, GEOMAR Helmholtz Centre for Ocean Research Kiel, Kiel, Germany, [3]College of Marine Science, University of South Florida, St. Petersburg, FL, United States

Fast repetition rate fluorometry (FRRf) based on active chlorophyll fluorescence is a powerful, noninvasive tool for studying phytoplankton physiological status at high spatial and temporal resolution. The South China Sea (SCS) is one of the largest tropical–subtropical marginal seas in the world, which plays an important role in modulating regional carbon budget and climate. In this study, underway *in situ* FRRf measurements were carried out throughout the outer continental shelf of the northern SCS, the basin of the northern SCS, the cyclonic eddy influenced domain in the western SCS, and the basin of the southeastern SCS. Pronounced diurnal variability of FRRf-derived parameters were observed, characterized by a large midday depression and slight nocturnal depression of the maximum quantum yield of photosystem II (F_v/F_m) and a slight increase in the functional absorption cross-section of photosystem II photochemistry (σ_{PSII}) at noon. F_v/F_m at the surface was typically as low as 0.1–0.3 and exhibited higher values (~0.4) where internal waves occurred. The cyclonic eddy increased F_v/F_m slightly, implying that it had a limited impact on surface phytoplankton photophysiology. With proper interpretation, FRRf has been a powerful tool to assess the physiological status of phytoplankton in the sea and to correlate that to ocean dynamics in an unprecedented fine scale.

KEYWORDS

diel variation, fast repetition rate fluorometry, photoinhibition, nutrient limitation, South China Sea, eddy

1 Introduction

Phytoplankton account for around half of global primary production (PP) and play an important role in regulating carbon cycling and climate (Longhurst et al., 1995; Falkowski et al., 1998; Field et al., 1998). In contrast to conventional methods requiring water sampling and incubation (e.g., incubation with ^{14}C tracer), fast repetition rate fluorometry (FRRf) (Kolber et al., 1998) is an active chlorophyll-*a* (Chl*a*) fluorescence technique rapidly probing phytoplankton physiological and bio-optical parameters *in situ* (Kolber and Falkowski, 1993; Behrenfeld and Kolber, 1999; Behrenfeld et al., 2006; Suggett et al., 2009; Schuback and Tortell, 2019; Zhu et al., 2022). There is significant potential to use FRRf signals to extend observations to much finer spatial and temporal scales than achievable with conventional techniques (Hughes et al., 2018). However, FRRf-derived signals are the result of the interacting influence of both the phytoplankton communities present and their physiological status, which in turn is impacted by environmental forcing (Suggett et al., 2009; Behrenfeld and Milligan, 2013). Their interpretation is therefore not always straightforward, and there is a need for more studies measuring ancillary biological and environmental parameters alongside FRRf in order to deconvolve these signals (Suggett et al., 2009; Behrenfeld and Milligan, 2013).

Phytoplankton growth in the ocean is frequently limited by nutrient availability, particularly in the sunlit surface waters of the low latitude oceans (Moore et al., 2013). Chlorophyll fluorescence measured by FRRf appears to be highly sensitive to nutrient limitation status, with limitation by either iron (Fe) and/or nitrogen (N)—the main limiting nutrients in the current ocean (Moore et al., 2013)—strongly regulating FRRf-derived parameters (Behrenfeld and Milligan, 2013). Specifically, at dawn and dusk when non-photochemical quenching (NPQ) processes are relaxed, values of the maximum quantum yield of photosystem II (PSII), F_v/F_m, are typically elevated under low N conditions and depressed under elevated N, low Fe conditions (Behrenfeld et al., 2006; Moore et al., 2008; Browning et al., 2014). Furthermore, in the tropical oceans under conditions of low Fe in combination with either low or elevated N, F_v/F_m values have been observed to show night time decreases from dusk to dawn (Behrenfeld and Kolber, 1999). This has been suggested to be due to cyanobacteria using their photosynthetic apparatus for respiratory electron transfer at night (Campbell et al., 1998), which, under low Fe conditions, leads to a strongly reduced plastoquinone (PQ) pool due to the restricted availability of Fe-rich photosystem I and cytochrome b6f proteins relative to the lower Fe PSII (Behrenfeld et al., 2006; Schrader et al., 2011). Night time reductions of σ_{PSII} also reflect increased night time reduction in the PQ pool under low Fe conditions (Behrenfeld and Kolber, 1999). Conversely, under Fe replete, N-limited conditions, nocturnal reductions in F_v/F_m and functional absorption cross-section of PSII photochemistry (σ_{PSII}) are much smaller or absent (Behrenfeld et al., 2006). Therefore, in addition to discrete measurements of F_v/F_m and σ_{PSII} made at any given time point, diurnal patterns in continuous active chlorophyll fluorescence could provide rich information for mapping nutrient stress status, specifically *via* distinguishing Fe, N, or N–Fe (co-)limitations (Behrenfeld and Milligan, 2013).

Independent of nutrient limitation, changes in F_v/F_m can also be related to phytoplankton community structure, with smaller values of F_v/F_m linked to increased antenna size of PSII, which has been found to be the case for small eukaryotic phytoplankton relative to large species in laboratory cultures (Suggett et al., 2009). Furthermore, strong decreases in F_v/F_m are associated with elevated light levels (reflecting light intensity that exceeds photosynthetic demand) (Wei et al., 2020). The suit of mechanisms downregulating F_v/F_m at elevated light levels are collectively termed non-photochemical quenching (NPQ), which can be reversed over timescales of seconds to hours upon exposure of phytoplankton to darkness (Falkowski and Raven, 2007).

The South China Sea (SCS) is the largest marginal sea of the North Pacific. Mesoscale physical processes, such as eddies, occur frequently in different parts of the SCS, significantly impacting nutrient distributions and carbon cycling (Xiu et al., 2010; Xiu and Chai, 2011; Jiao et al., 2014; Li et al., 2017; Zhang et al., 2020). These physical processes result in distinct patterns of phytoplankton community structure (Huang et al., 2010; Wang et al., 2016; Wang et al., 2018), PP (Ning et al., 2004; Liao et al., 2021) and supposedly physiology (Liao et al., 2021). Cyclonic eddies (CEs) occur frequently during summer in the western SCS, driving a shoaling of the nitracline depth to as shallow as 20 m relative to ~70 m in the background state (Jiao et al., 2014). Chl*a* biomass of diatoms and *Synechococcus* alongside overall rates of PP have been observed to rise significantly inside CE as a consequence of enhanced nutrient supply (Wang et al., 2016; Liao et al., 2021). In contrast, the effects of anticyclonic eddies (ACEs) on phytoplankton community structure are more diverse, with ACE leading to convergence of low nutrient surface waters leading to the community structure inside ACE being similar to that of surrounding waters (Huang et al., 2010). In addition, sub-mesoscale upwelling at the edge of ACE has been shown to drive a modest effect of increasing the Chl*a* biomass of diatoms and haptophytes (Wang et al., 2018).

So far, studies of eddies in the SCS accompanying measurements of photophysiology have not been made. However, other studies have indicated that nutrient availability impacts photophysiology in this region (Jin et al., 2016; Xie et al., 2018). Using diel FRRf measurements, Jin et al. (2016) investigated phytoplankton physiology at local noon in the northern SCS, showing decreasing F_v/F_m values from the coast

to central basin and increasing values from the surface to deep. Furthermore, Xie et al. (2018) measured the diel cycle of F_v/F_m for a natural assemblage of *Prochlorococcus*, the most abundant phytoplankton class in the SCS, and related the observed diel variability to nutrient stress. Here, we undertook an FRRf survey over a much larger area of the SCS than in these previous studies, ranging from the outer continental shelf to the entire basin and crossing CE and ACE features, and complementing these measurements with diagnostic pigment analyses to aid with deconvolving nutrient, community, and light effects on F_v/F_m and σ_{PSII}.

2 Materials and methods

2.1 Underway FRRf measurements

Observations were made during cruise KK1808 onboard the R/V *Tan Kah Kee* (18 September–14 October 2018). Underway FRRf measurements were conducted with a FastOcean coupled with an Act2 Laboratory System (Chelsea Technologies, UK). The ship's underway system collected seawater continuously from a depth of ~5 m, which then transitioned through a ~50-m dark pipe before flowing into the Act2 System. The dark acclimation period from water entering the vessel to FRRf measurement was estimated to last approximately 5 min, which is similar to that of Behrenfeld and Kolber (1999). The FRRf was set to perform acquisitions using 100 blue excitation (450 nm) flashlets with 2-ms intervals. Fluorescence transients were fit within the manufacturers' software (ActRun) to yield the initial fluorescence yield (F_o), maximum fluorescence yield (F_m), and σ_{PSII}. Blank fluorescence of deionized water (Milli-Q) samples was subtracted from raw F_o and F_m values and F_v/F_m recalculated.

2.2 Continuous shipboard measurements and satellite data products

Time and geographic coordinates were recorded by the shipboard geographical positioning system (GPS). The time was converted to local time, allowing alignment of light–dark periods. Sea-surface temperature (SST) and salinity were continuously measured by an SBE21 CTD (Sea-Bird Electronics, USA). The FastOcean plus Act2 Laboratory System measured fluorescence-based chlorophyll *a* concentrations ($Chla^{FRRf}$), which was then calibrated against high-performance liquid chromatography (HPLC)-determined concentrations of chlorophyll *a* pigments. To characterize the mesoscale eddies in the study area, daily, 1/4° gridded sea level anomaly (SLA) data between 8 September and 14 October 2018 were downloaded from the Copernicus Marine and Environment Monitoring Service (CMEMS) (available from: http://marine.copernicus.eu/). In addition, a 10-min resolution instantaneous photosynthetically available radiation (iPAR, µmol quanta m^{-2} s^{-1}) was extracted from Himawari-8 level 2 products (available from: https://www.eorc.jaxa.jp/ptree/), and daily integrated surface PAR data (mol quanta m^{-2} day^{-1}) were extracted from the standard MODIS-Aqua Level-3 products at 4-km pixel resolution (available from: http://oceancolor.gsfc.nasa.gov/). Each *in situ* underway measurement was matched with a daily SLA, iPAR, and PAR dataset using the closest pixel of the respective satellite products. Himawari-8-derived iPAR values were consistent with *in situ* measurement derived from PAR sensor mounted in the CTD with p <0.01 and r =0.87 (Supplementary Figure S1).

2.3 Pigments and chemotaxonomic analysis

Seawater samples were collected with Niskin bottles from discrete depths at the stations (Figure 1). Seawater (4–6 L) at

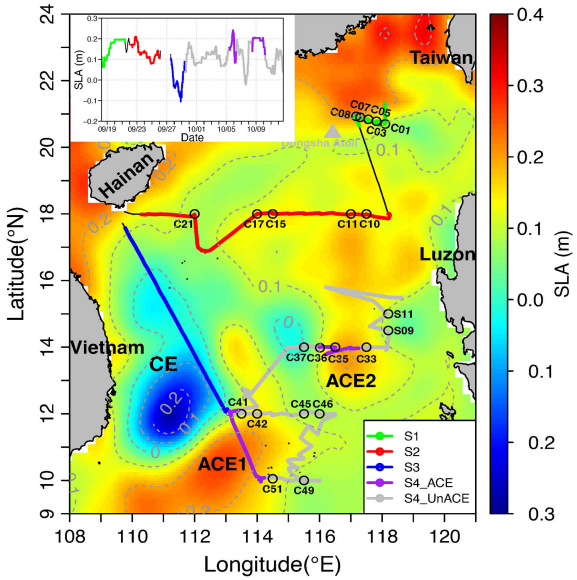

FIGURE 1
Map of sampling stations based on the average sea level anomaly (SLA) from 18/09/2018 to 14/10/2018. The top left box indicates the matched daily sea level anomaly (SLA) of the cruise track. The black dots were stations with phytoplankton pigment survey during the cruise. The color lines were the cruise track, which can be divided into four transects: S1 was selected as the continental shelf of northern SCS; S2 referred to the basin of northern SCS; S3 located in the western SCS where cyclonic eddies occurred; S4 distributed in the basin of southeastern SCS. CE, cyclonic eddy; ACE, anticyclonic eddy. S1, S2, S3, S4_ACE (through ACE1 and ACE2), and S4_UnACE (outside ACE1 and ACE2) were in green, red, blue, purple, and gray, respectively.

each depth was filtered onto a 25-mm diameter GF/F glass fiber filter under gentle vacuum (<75 mmHg) and stored in liquid nitrogen until analysis. In the laboratory, filters were immersed in N, N-dimethylformamide for pigment extraction. Extracts were analyzed with an UltiMate 3000 HPLC system (Thermo Fisher Scientific, USA) calibrated with pigment standards (DHI Water & Environment, Denmark) following the procedure of Furuya et al. (2003).

Thirteen pigments detected included chlorophyll *c*2, chlorophyll *c*3, peridinin, 19'-butanoyloxyfucoxanthin, fucoxanthin, neoxanthin, prasinoxanthin, 19'-hexanoyloxyfucoxanthin, violaxanthin, diadinoxanthin, alloxanthin, diatoxanthin, zeaxanthin, lutein, chlorophyll *a*, chlorophyll *b*, divinyl chlorophyll *a*, α-carotene, and β-carotene. CHEMTAX software was then used to estimate the contribution of different phytoplankton groups to total chlorophyll *a* (the sum of chlorophyll *a* and divinyl chlorophyll *a*) (Mackey et al., 1996). The initial input matrix of ratios of diagnostic pigments to total chlorophyll *a* was identical to the input matrix used in previous studies in the South China Sea (Wang et al., 2015; Xiao et al., 2018). Successive runs were done for each group to gain convergence between input and output ratios according to the CHEMTAX protocols described by Latasa (2007). Nine phytoplankton groups were computed, including Dinoflagellates (Dino), Diatoms (Diat), Type-8 Haptophytes (Hapt_8), Type-6 Haptophytes (Hapt_6), Cryptophytes (Cryp), Chlorophytes (Chlo), Prasinophytes (Pras), *Synechococcus* (*Syne*), and *Prochlorococcus* (*Proc*), and we used only surface phytoplankton information in this study. In addition, the carotenoids were separated into photosynthetic carotenoids (PSCs) and photo-protective carotenoids (PPCs). The former includes peridinin, 19'-butanoyloxyfucoxanth, fucoxanthin, and 19'-hexanoyloxyfucoxanthin. The latter includes violaxanthin, diadinoxanthin, alloxanthin, diatoxanthin, zeaxanthin, ββ- + βε-carotene, and lutein (Barlow et al., 2007).

2.4 Statistical analysis

A one-way ANOVA was used for statistical analysis to compare the difference between environmental and FRRf-derived parameters among sections, Tukey's HSD test was performed for post-hoc test for multi-comparisons. In order to deconvolve light signal and other factors for F_v/F_m, a simple model was constructed. In the model, F_v/F_m is a linear function of iPAR, and the constant of the linear function represents influence of other factors together, but different regions have different constants for their own nutrient conditions; in addition, a two-way ANOVA was conducted in the beginning and determined that both light and region were significant factors and the slope of the linear function is invariant for different regions (because of no interaction effect between light and region, Supplementary Table S1). All statistical analyses were performed using open source statistical software R version 3.6.0 (R Development Core Team, 2016). Figures were plotted using Ocean Data View 5 (Schlitzer, 2019) and R software.

3 Results

Clear variations in hydrographic properties and SLA during the cruise were observed (Figures 1, 2). Chlorophyll fluorescence was relatively elevated in the northern SCS continental shelf transect selected as S1. Relatively lower SST and higher salinity were observed around 18° SCS and was named S2. SLA images identified the positions of one cyclonic eddy (CE) and two anticyclonic eddies (ACEs, ACE1, and ACE2) that our cruise passed through. Accordingly, we then classified S3, S4_ACE, and S4_UnACE (regions outside of the eddies in S4) into different water masses in the western and southeastern SCS (Figure 1). A principal component analysis (PCA) was performed to segment the underway dataset based on biological and environment factors (Figure 3). The first two principal components

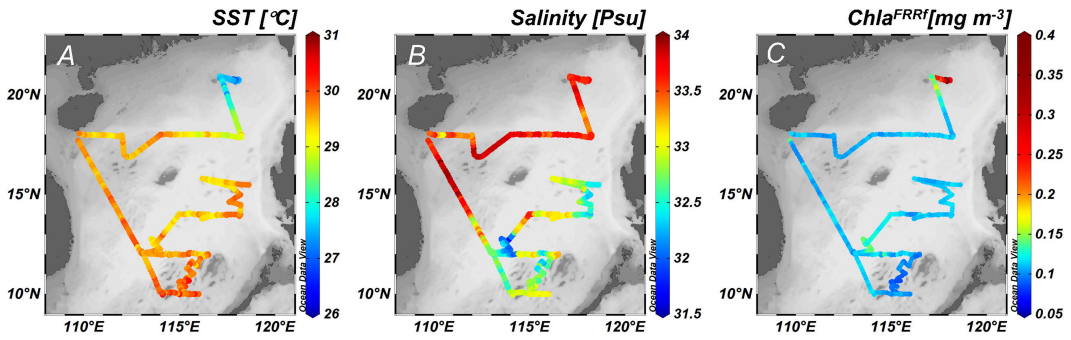

FIGURE 2
Underway surface sea temperature (SST) **(A)**, surface salinity **(B)**, and surface fluorescence ($Chla^{FRRf}$) **(C)** during the cruise.

accounted for more than 60% of the total variation, with the first principal component driven by variations in temperature and chlorophyll fluorescence and the second by SLA (Figure 3). The groups distinguished based on chlorophyll fluorescence, SST, and SLA accordingly separated within PC1–PC2 space.

3.1 The shelf edge of the northern SCS (Section S1)

Section S1 was located at the edge of the northern continental SCS shelf close to the Dongsha Atoll (Figure 1). Section S1 had the lowest SST and highest Chla^{FRRf} of the survey (Figure 2; Table 1). Ranges of SST and Chla^{FRRf} along this section varied from 26.7°C to 28.0°C and from 0.12 to 0.51 mg m^{-3}, respectively, but salinity showed small variability (33.4–33.76 psu; Figures 2, 5). Phytoplankton compositions in this region were also distinct, with higher proportions of Prasinophytes (6%–15%) ($p < 0.01$), Type-8 Haptophytes (9%–19%) ($p < 0.01$), and Diatoms (0%–15%) ($p < 0.05$) and lower proportions of *Prochlorococcus* (18%–30%) ($p < 0.05$) than the other sections (t-test for significantly different means; Figure 4). Between stations C01 and C03, SST declined by ~0.8°C, and Chla^{FRRf} showed a synchronous peak (Figure 5C). Although C03 was not at the center of SST minimum, Chla^{HPLC} was the highest observed (0.4 mg m^{-3}), and the diatom percentage contribution to total chlorophyll-a was also the highest for the cruise (15%). Following C03, Chla^{HPLC} gradually decreased landwards, while the proportions of Prasinophytes and Diatoms decreased but *Synechococcus* and *Prochlorococcus* increased (Figure 4).

A peak of F_v/F_m up to 0.40 matched the SST minimum, closely corresponding with Chla^{FRRf} (Figure 5C). Besides this peak, F_v/F_m values were relatively low (<0.3). The PSII functional absorption cross-section (σ_{PSII}) remained relatively constant (mean of 701 Å^2; Figure 5C). Generally, F_v/F_m exhibited maxima at sunrise (~0.30) and sunset (~0.24) with depressions at midday (~0.20) and at about 22:00 (~0.27). By contrast, diel variability in σ_{PSII} (615–870 Å^2) was relatively minor although demonstrated an afternoon increase (Figure 5E).

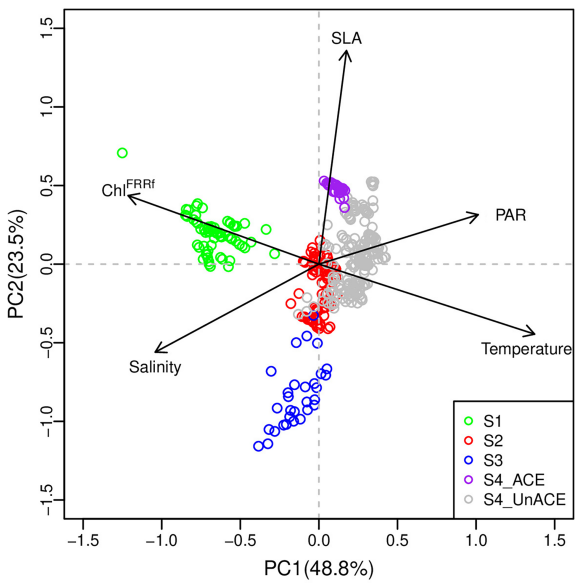

FIGURE 3
Principle component analysis (PCA) of matched underway biological and environment factors during the cruise. S1, S2, S3, S4_ACE (through ACE1 and ACE2), and S4_UnACE (outside ACE1 and ACE2) were dots in green, red, blue, purple, and gray, respectively.

3.2 The northern basin (Section S2)

Section S2 defined the 18°N transect from 118°E to 110°E (Figure 1). SLA showed higher values in the eastern part of the transect, contrasting with lower values around C21 (Figure 1). SST between 28.7°C and 30°C was observed and increased gradually during the daytime in the area until reaching 114°E (Figure 6). Salinity increased generally from 33.5 to 33.9 psu until a sharp drop to 33.3 psu before the station C21 and then a further reduction to 33.0 near Hainan Island (Figures 2, 6B). Both Chla^{FRRf} (0.10–0.12 mg m^{-3}) and Chla^{HPLC} (~0.08 mg m^{-3}) were lower than S1 (Figure 6C, Table 1), and phytoplankton compositions were *Synechococcus* (37%–57%) and *Prochlorococcus* (32%–51%) dominated (Figure 4).

Compared with Section S1, F_v/F_m (0.10–0.30) and σ_{PSII} (416–799 Å^2) values in S2 were significantly lower ($p < 0.01$) (Table 1). However, the fluctuation of diel patterns of F_v/F_m in S2 were more pronounced, showing lower peaks at sunrise (~0.27) and sunset (~0.23) and pronounced midday (~0.14) and more modest night time (~0.20) reductions (Figure 6D). Furthermore, σ_{PSII} showed a clear diel pattern, with a pronounced midday maximum that was approximately 1.4-fold higher than night time values (Figure 6E).

3.3 The eddy domain of the western SCS (Section S3)

Section S3 started from Hainan Island heading southeast, intersecting the edge of a cyclonic eddy to the east of Vietnam (Figure 1). Along this section, SLA were depressed (−0.07–0.13 m), and within the vicinity of the cyclonic eddy, SST ranged 29.3°C–30°C (Table 1; Figure 7B). Chla^{FRRf} remained relatively constant (~0.10 mg m^{-3}) (Figure 7C; HPLC samples not collected).

Values of F_v/F_m were significantly higher than S2 and S4 ($p < 0.01$), varying between 0.14 and 0.32 in the cyclonic eddy (Table 1). F_v/F_m showed a clear diel pattern, with higher

TABLE 1 Mean ± SD of surface environment conditions and FRRf-derived parameters performance in the SCS along the cruise.

Location	Northern SCS		Western SCS	South Eastern SCS	
N	Shelf (S1) 95	Basin (S2) 130	CE (S3) 57	ACE1 and ACE2 (S4) 84	Outside ACE1 and ACE2 (S4) 318
Temperature (°C)	27.38 ± 0.28^{a}	29.32 ± 0.28^{b}	29.68 ± 0.17^{c}	29.53 ± 0.26^{d}	29.66 ± 0.28^{c}
Salinity (psu)	33.64 ± 0.08^{a}	33.61 ± 0.21^{a}	33.38 ± 0.46^{b}	32.98 ± 0.21^{c}	32.72 ± 0.37^{d}
Chla^{FRRf} (mg m^{-3})	0.24 ± 0.10^{a}	0.11 ± 0.01^{b}	0.11 ± 0.01^{b}	0.11 ± 0.01^{b}	0.11 ± 0.01^{b}
SLA (m)	0.12 ± 0.04^{a}	0.13 ± 0.03^{a}	0.01 ± 0.05^{b}	0.21 ± 0.04^{c}	0.13 ± 0.04^{a}
PAR (mol quanta m^{-2} day^{-1})	41.70 ± 6.91^{a}	52.45 ± 3.07^{b}	44.29 ± 7.02^{a}	52.92 ± 0.58^{b}	52.65 ± 4.46^{b}
F_v/F_m	0.23 ± 0.06^{a}	0.20 ± 0.04^{b}	0.24 ± 0.04^{a}	0.15 ± 0.05^{c}	0.17 ± 0.05^{d}
F_v/F_m *(T=dawn)*	0.29 ± 0.07^{a}	0.26 ± 0.03^{a}	0.27 ± 0.03^{a}	0.18 ± 0.04^{b}	0.21 ± 0.05^{b}
F_v/F_m *(T=midnight)*	0.27 ± 0.05^{a}	0.21 ± 0.02^{b}	0.23 ± 0.02^{ab}	0.16 ± 0.04^{c}	0.17 ± 0.04^{c}
F_v/F_m *(T=noon)*	0.17 ± 0.05^{a}	0.14 ± 0.02^{ab}	0.18 ± 0.02^{a}	0.09 ± 0.01^{c}	0.13 ± 0.04^{b}
σ_{PSII} (Å^2)	714 ± 70^{a}	547 ± 77^{b}	508 ± 41^{c}	437 ± 101^{d}	484 ± 77^{c}

The superscript labels a–d implied significant difference at the level of $p < 0.05$ using one-way ANOVA (SLA, sea level anomaly; PAR, daily integrated photosynthetically available radiation at the surface).

sunrise (~0.29), sunset (~0.29), and lower midday (~0.17) and night (~0.23) values (Figure 7D; Table 1). Values of σ_{PSII} remained relatively constant (421–587 Å^2) in the cyclonic eddy, with a small increase around midday (Figure 7E).

3.4 The southeastern basin (Section S4)

This section intersected anticyclonic eddies ACE1 and ACE2 (S4_ACE) with regions outside of the eddies defined as S4_UnACE (Figure 1). Salinity varied between 32.0 and 33.3 psu and SST between 29.2°C and 30.6°C. The map showed that this section, particularly outside the ACEs, was characterized by the lowest salinity among all sections (Figure 2B). Chla^{FRRf} remained relatively constant (0.11–0.12 mg m^{-3}) but increased (~0.14 mg m^{-3}) on the outside of ACE1 associated with a salinity decrease (~32.0 psu). Two abrupt changes in Chla^{FRRf} were observed at the edge of ACEs, with Chla^{FRRf} increasing by ~0.03 mg m^{-3}. Across ACE2, SST and salinity were relatively constant (29.3°C–29.7°C; salinity, ~33.1 psu), while Chla^{FRRf} gradually declined from 0.14 to 0.10 mg m^{-3} (Figure 8). *Synechococcus* and *Prochlorococcus* together were the largest contributor to Chl*a* throughout (Figure 4).

Ranges of F_v/F_m inside and outside the ACEs were 0.07–0.26 and 0.07–0.32, respectively. Smoothed F_v/F_m curves showed that the sunrise (~0.19) and sunset values (~0.17) inside the ACEs were similar with those outside (~0.21 and ~0.19), but those curves overlooked spatial variations. For example, the ACE1 had apparent higher sunrise and sunset F_v/F_m than the ACE2. Nevertheless, the smoothed curves did capture the midday minimum (0.09 ± 0.01) inside the ACEs, which was lower than those outside (0.13 ± 0.04) (Figure 8D; Table 1). The values of σ_{PSII} were the lowest of the cruise and varied between 64 and 663 Å^2 (Table 1), and the diel patterns showed a small increase in σ_{PSII} in the afternoon both inside and outside ACEs (Figure 8E).

3.5 Comparisons between and within sections

Section S1 was distinct to other sections and characterized by lower SST of 27.4 ± 0.3°C and higher Chla^{FRRf} of 0.24 ± 0.10 mg m^{-3} (Table 1). Section S1 was heterogeneous with the abrupt bump of F_v/F_m at the first night (Figure 5). Sections S2 and S3 were relatively homogeneous; F_v/F_m were consistently higher in Section S3 than those in Section S2, although the differences were quantitatively small (Table 1). Moreover, σ_{PSII} in Section S2 had a significant increase in the afternoon, which was not apparent in Section S3 (Figure 6). The average dawn F_v/F_m of sections S1–S3 were all smaller than 0.3 (0.26–0.29) but still higher than that in Section S4 (0.18 and 0.21 inside and outside ACEs, respectively). Corresponding to similar iPAR at noon, ACEs revealed significantly lower noon F_v/F_m (0.09 ± 0.01) than that of S4_UnACE. In general, F_v/F_m experienced <20% reduction at midnight but up to 50% at noon, by using the dawn value as the reference.

4 Discussion

Our results of the active fluorescence measurements in the SCS may reflect diurnal variations in FRRF-derived parameters and spatial changes in photophysiology of phytoplankton assemblages and their taxonomic compositions related to environmental forcing (Behrenfeld et al., 2006; Suggett et al., 2009). Therefore, it was

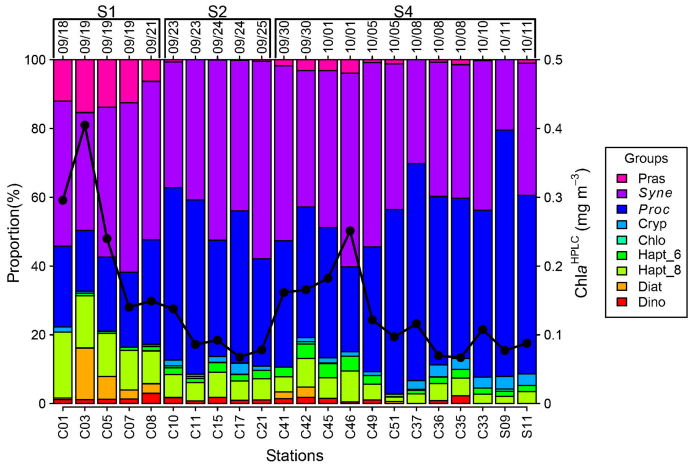

FIGURE 4
The concentration of total Chl *a* ($Chla^{HPLC}$) and contributions of different phytoplankton groups during the cruise. Dino, Diat, Hap_8, Hap_6, Chlo, Cryp, *Proc*, *Syne*, and Pras are the abbreviations for Dinoflagellates, Diatoms, Haptophytes (type 8), Haptophytes (type 6), Chlorophytes, Cryptophytes, *Synechococcus*, *Prochlorococcus*, and Prasinophytes.

challenging to compare any instantaneous F_v/F_m measurement between regions (Supplementary Figure S2). We first discuss the influence of phytoplankton composition on FRRF-derived parameters and typical diurnal patterns over the entire SCS, followed by a discussion on effects of mesoscale eddy structure on phytoplankton photophysiology within the SCS.

4.1 Challenge 1: Understudied photophysiology of prokaryotic phytoplankton

Suggett et al. (2009) showed from active fluorescence data for phytoplankton cultures in previous studies that there was a negative relationship between (optimal) F_v/F_m and σ_{PSII} across

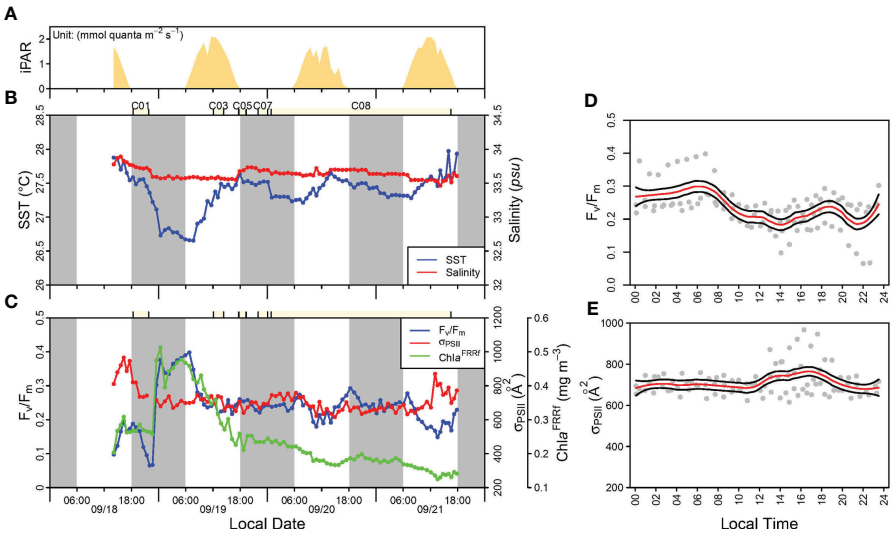

FIGURE 5
The incident irradiance **(A)**; environment conditions including SST and salinity **(B)**; F_v/F_m, σ_{PSII}, and $Chla^{FRRf}$ **(C)**; diel pattern of F_v/F_m **(D)**; and diel pattern of σ_{PSII} **(E)** for the continental shelf of the northern SCS (Section S1). Light yellow, white, and gray-shaded area indicate the HPLC sample station and local daytime and nighttime, respectively. The red lines in panels **(D)** and **(E)** are smoothed using the loess method (span = 0.3), while the black lines represent the regression values ± SE.

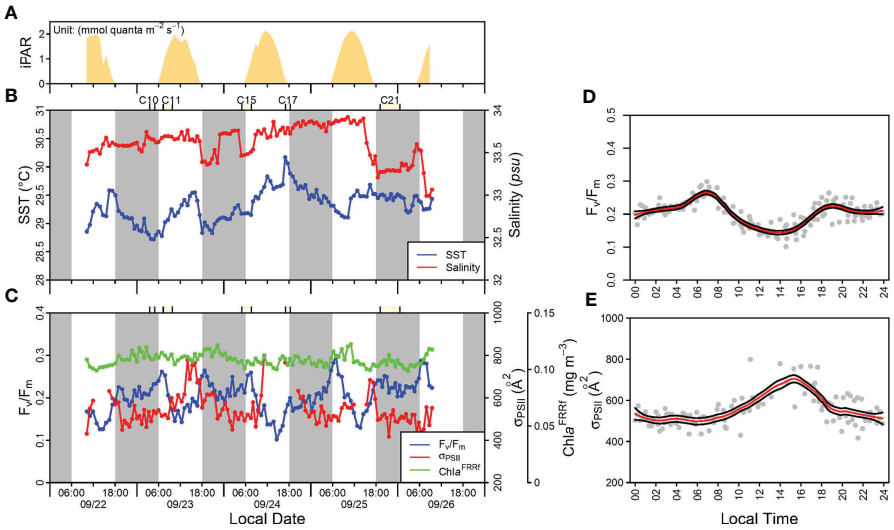

FIGURE 6
Same as Figure 5 but for basin of the northern SCS (Section S2).

eukaryotic taxa. The relationship was explained by the distinct light absorption and excitation energy transfer for each taxon and their energetic interpretation, which were likely related to selective pressure during phytoplankton evolution. However, in this study, no relationship was found between the two measurements (Figure 9A) despite that bulk σ_{PSII} actually reflected the relative amount of light-harvesting pigments (which was governed by phytoplankton composition) (Figures 9B, C). Assuming that F_v/F_m of eukaryotic phytoplankton in the SCS was also taxonomic dependent, perhaps the lack of a negative relationship was due to the contribution by both FRRF parameters from *Synechococcus* predominated in the SCS surface waters. This is because *Synechococcus* have relatively low σ_{PSII} (at blue excitation waveband) and F_v/F_m, attributed to their light absorption maxima being more shifted to "green" and the fluorescence from their relatively abundant PSI and phycocyanin, which disturbs PSII fluorescence signal (Raateoja et al., 2004). On the

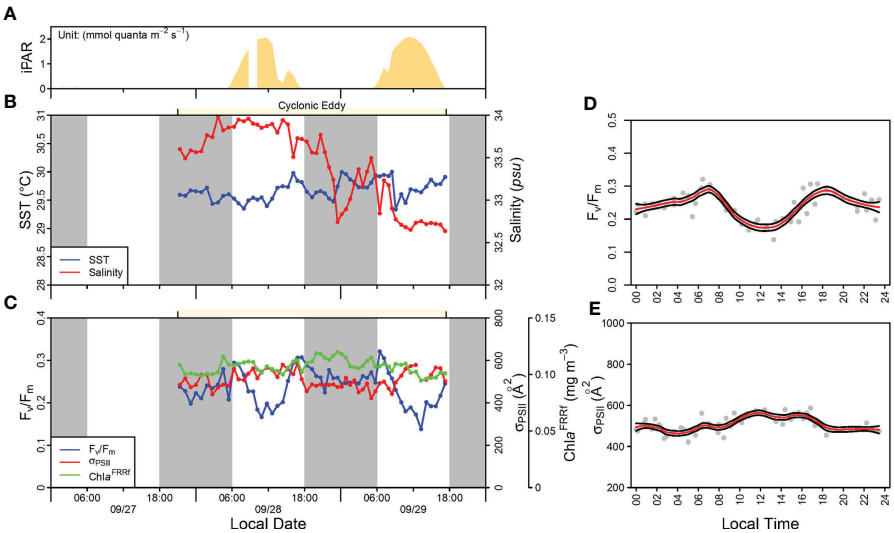

FIGURE 7
Same as Figure 5 but for eddy domains in the Western SCS (Section S3).

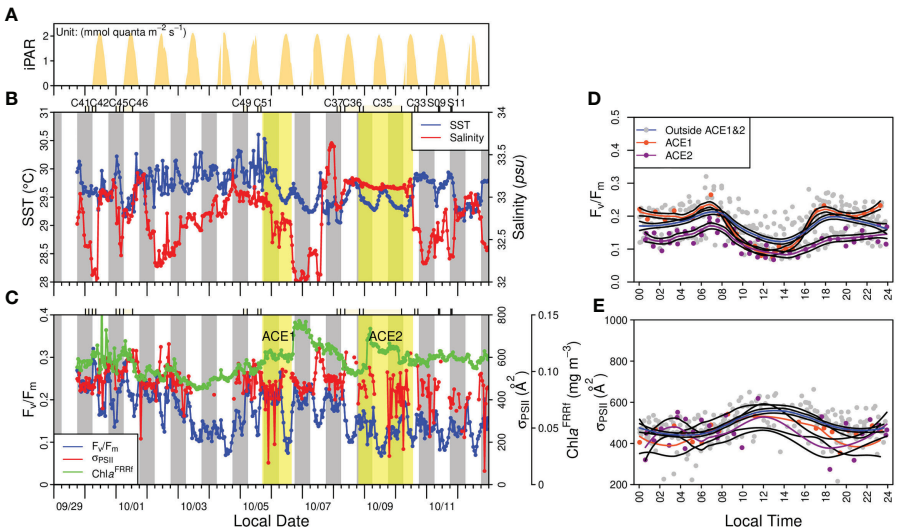

FIGURE 8
Same as Figure 5 but for the basin of the southeast SCS (Section S4).

other hand, *Prochlorococcus*, another dominant species of SCS, has been reported to have different F_v/F_m and σ_{PSII} than *Synechococcus* (Raateoja et al., 2004; Six et al., 2007; Suggett et al., 2009), probably due to distinct pigment compositions with predominantly divinyl chlorophyll (Ting et al., 2002). In any case, the lack of a negative F_v/F_m versus σ_{PSII} relationship as expected from taxonomic changes for eukaryotic phytoplankton was partly due to the dominance of *Synechococcus*, whose parameters do not follow it.

Meanwhile, the low drawn F_v/F_m below 0.3 may be related to the dominance of *Synechococcus*. This is because *Synechococcus* are known to overexpress iron-stress-induced chlorophyll binding protein IsiA under Fe-limited conditions, whereby the extra fluorescence from the IsiA supercomplexes detached to reaction centers would reduce apparent F_v/F_m (Schrader et al., 2011). Antenna proteins similar with IsiA are also found in low-light ecotypes of *Prochorococcus* (Bibby et al., 2003). However, this hypothesis of Fe deficiency in surface waters of the SCS basin appears unlikely, as the measured nitrate concentrations were 0.002–0.2 μM and previously reported Fe concentrations for this region were 0.2–0.3 nM (Wu et al., 2003; Wen et al., 2022), by assuming a threshold of 10:1 N:Fe ratio (μM:nm) for Fe limitation (Browning et al., 2017). Perhaps more likely is that absolute values of F_v/F_m are influenced by the active fluorescence measurement protocol and the instrument used and as such should be evaluated with caution (as discussed in ***Section 4.2***).

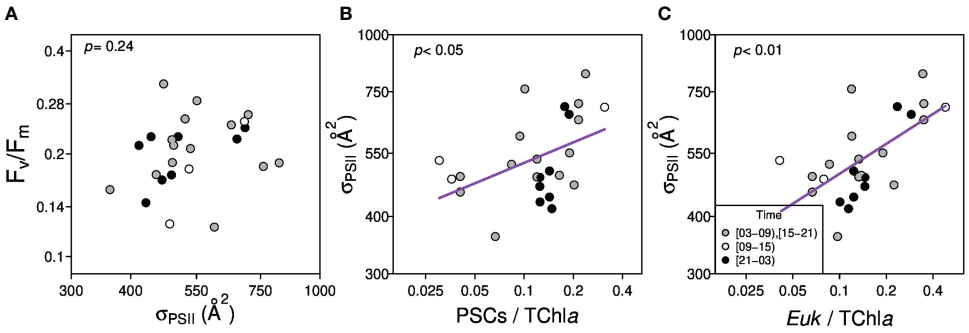

FIGURE 9
The relationship between F_v/F_m and σ_{PSII} **(A)**; σ_{PSII} and photosynthetic carotenoids (PSCs)/TChl *a* **(B)**; σ_{PSII} and *Euk*/TChl a **(C)**. The color represents the time period with the legend in panel (**C**). *Euk* was short for eukaryotic phytoplankton.

4.2 Challenge 2: Widespread diel pattern of F_v/F_m throughout the SCS

Diel variability of F_v/F_m was observed throughout the SCS, with midday minima, maxima at dawn and dusk, and a slight nocturnal decrease (Figures 5–8). This pattern has been observed previously in the central SCS (Xie et al., 2018) and the coastal SCS (Xu et al., 2020; Mai et al., 2021) and several other studies elsewhere in the tropical ocean (Behrenfeld et al., 2006; Mackey et al., 2008; Doblin et al., 2011; Browning et al., 2017). The magnitude of midday minima can vary with incident PAR at noon and the duration of dark acclimation. In this study, the 5-min dark acclimation did not provide sufficient time for phytoplankton to relax the slow NPQ components, which could last for tens of minutes to hours. Furthermore, any repair of damaged PSII reaction centers also requires longer timescales. The sustained quenching to chlorophyll fluorescence led to a lower dark-acclimated F_m and F_v/F_m than it would be with a longer dark acclimation timescale (Supplementary Figure S3). The decline in F_v/F_m relative to its dawn value was positively correlated with the incident PAR (Supplementary Figure S4), suggesting the photoprotective nature of NPQ.

In general, it is expected that the nocturnal reduction in F_v/F_m is due to PQ pool reduction by "chloro-respiration" in the dark and is thought to depend on the degree of Fe stress that would deplete photosynthetic components [such as cytochrome b6f and photosystem I (PSI)] on the accepter side of the electron transfer chain (Behrenfeld and Milligan, 2013). The nocturnal reduction in the SCS was up to ~20% (in Section S4), which is smaller than the nocturnal reduction of >25% seen in Fe-limited surface waters in the equatorial Pacific reported by Behrenfeld et al. (2006). This may suggest that phytoplankton growth in the SCS was not severely Fe limited. Behrenfeld et al. (2006) also used dawn F_v/F_m maxima in combination with nocturnal reduction to delineate three ecophysiological regimes in the tropical Pacific (iron sufficient with low macronutrients, iron limited with low macronutrients, and iron limited with elevated macronutrients). Following their diagnostic diagram [Figure 4 in Behrenfeld et al. (2006)], our SCS data did not belong to any of those three since dawn F_v/F_m was <0.45. While this could imply a substantial difference between the tropical Pacific and the SCS with respect to nutrient availability, such comparisons should be made with caution. This is because absolute values of F_v/F_m are highly dependent on active fluorescence measurement protocols and employed instrumentation. For example, our correction using blank fluorescence from deionized water instead of filtered seawater might have underestimated F_v/F_m measurements (Cullen and Davis, 2003). If the underestimation of F_v/F_m in this study was true, the categorization of the SCS should possibly be the regime "iron-sufficient with low macronutrients," consistent with the reported Fe and nitrate data in the SCS waters in literatures (Wu et al., 2003; Wen et al., 2022). Such speculation should be examined in future nutrient addition experiments.

4.3 Nutrient effects on phytoplankton physiology by cyclonic eddies

Nutrients are usually considered as the most important factor for the growth of phytoplankton in the SCS (Ho et al., 2015) and always depleted in the upper mixed layer in the oligotrophic water along with strong stratification during summer. In this study, as described above, F_v/F_m at the surface was typically as low as 0.1–0.3, and phytoplankton communities were dominated by *Synechococcus* and *Prochlorococcus* at the surface, indicating the oligotrophic condition in most of our study area during this cruise. Within the study area, it is expected that Section S3 region crossing the cyclonic eddy was pumped with some nutrients from the nutrient-rich deeper layer (McGillicuddy, 2016), and therefore, phytoplankton physiological status may have been more favorable. The F_v/F_m exhibited consistently higher values in Section S3 where CE occurred than in the preceding Section S2 ($p < 0.01$) (Figure 7; Table 1), but the increases (about 0.04) were small, and the diel variation remained the same (Figures 6, 7). The high SST of 29.5°C–30°C likely rejected the assumption of large amount of nutrient-rich water injected into the surface. At the same time, the Chla^{FRRf} values in Section S3 were about 0.11 mg m^{-3}, as similar as that in Section S2. Previous studies in the SCS showed both elevated nutrient inventory and Chl*a* in CE, but cold and nutrient-rich water was injected mainly into the lower part of euphotic zone. Chl*a* at the deep chlorophyll maximum layer could be increased to larger than 1 mg m^{-3}, which was more than double of the background concentration, but Chl*a* at the surface was rarely increased; the reported surface Chl*a* within cold eddies (normally 0.1–0.2 mg m^{-3}) was consistent with our observation (Jiao et al., 2014; Wang et al., 2016; Liao et al., 2021). Taken together, these results implied that the CE had limited impacts on the surface phytoplankton communities. On the contrary, small scale but large increases in F_v/F_m were observed in the shelf area. Section S1 adjoined the Dongsha Atoll, where internal waves were frequently detected (Hsu et al., 2000; Zhao et al., 2004; Liu et al., 2006; Pan et al., 2012) (Figure 1). The sudden drop of SST value, corresponding the higher Chla^{FRRf} than those in nearby subregion in this area, is consistent with previous studies and indicated the occurrence of the internal waves between the station C01 and C03 along this transect (Figures 2, 5). The dawn F_v/F_m of as high as 0.4 was accompanied by a Chl*a* concentration of about 0.4 mg m^{-3} and 15% contribution by diatoms at station C03. The results suggested that the F_v/F_m pattern observed in Section S1 was significantly affected by physical processes that can effectively supply nutrients to fuel phytoplankton growth. It also suggests that

this level of nutrient supply cannot be reproduced by physical processes associated with the mesoscale cyclonic eddy structure seen in Section S3. However, it should be noted that the change in F_v/F_m is usually disproportional to the change in carbon fixation; a study in the CE area of the western SCS but half month before this study found a twofold increase in the average Chl*a*-specific carbon fixation rate inside the CE than outside (Liao et al., 2021), with the implication being that FRRf could not probe any altered photosynthetic efficiency that does not occur at the intracellular site of PSII.

4.4 Effects of anticyclonic eddies on phytoplankton physiology

The lowest values of F_v/F_m were found in the southeast basin associated with ACE2 (Figure 8); these may be explained in the case of anticyclonic eddy based on the doming of its isopycnals and nutricline, therefore causing lower sustained phytoplankton biomass in this area (McGillicuddy, 2016). ACE1 was adjacent to the Mekong River plume area characterized by lower salinity of <32.5 psu, while ACE2 was located in the remote and more oligotrophic southeast basin. The river input provides nutrients to promote phytoplankton growth, and the dawn F_v/F_m in ACE1 was 0.24 (Figure 8D). Meanwhile, the ACE2 showed the lowest Chl*a* of 0.07 mg m^{-3} corresponding to a dawn F_v/F_m of 0.17. Huang et al. (2010) reported two ACEs in the northern SCS during wintertime with much more abundant eukaryotic phytoplankton in the ACE with entrainment of coastal water. These phenomena highlighted the effects of source water mass on phytoplankton in ACEs. However, the midday minimums of F_v/F_m were the same (~0.09) between the two ACEs (Figure 8D), with the phytoplankton in the ACE1 exhibiting higher light sensitivity than those in surrounding waters.

5 Conclusions

In this study, underway FRRf measurements were used to record high-resolution diel changes in F_v/F_m and σ_{PSII} throughout the SCS. Pronounced diurnal variability of both F_v/F_m and σ_{PSII} were observed, characterized by large midday depressions and slight nocturnal depressions of F_v/F_m, and slight increases in σ_{PSII} at noon, which was especially pronounced under expected elevated nutrient stress conditions. Slightly but consistently higher F_v/F_m throughout the day in the western SCS compared to the northern SCS basin suggested the potential role of cyclonic eddies in partially relieving nutrient stress. Apparent increase in F_v/F_m occurred only in a shelf area influenced by internal waves, where we hypothesized that nutrients were injected into surface waters. The two ACEs exhibited different dawn, dusk, and night time values of F_v/F_m, indicating effects of source water mass on phytoplankton photophysiology. We recommend that future studies investigating phytoplankton photophysiology in the SCS should focus on more detailed mechanisms (e.g., vertical structure of mesoscale eddies, any other mesoscale process, and typhoon) possibly *via* nutrient addition experiments conducted over different timescales to directly test the impact of nutrient supply on phytoplankton photophysiology.

Data availability statement

The raw data supporting the conclusions of this article will be made available by the authors, without undue reservation.

Author contributions

HL, YX, and BH conceived this study. HL and FX conducted the sample collection and analysis. HL drafted the original manuscript. YX and TJB critically reviewed and edited the manuscript. All authors contributed to the article and approved the submitted version.

Funding

This work was supported by the National Natural Science Foundation of China through grants 42130401 and 42141002.

Acknowledgments

We thank Yin-Ning Zhang who is very gentle to lend us FastOcean plus FastAct, and Gai-Lian Li for her support on cruise preparation. We also thank NSFC Shiptime SharingProject (41749906) for supporting the cruises by R/V *Tan Kah Kee* (No. NORC2018-06). We also thank the captain and crew of R/V *Tan Kah Kee* for their tremendous helps during the cruise. We also thank the reviewers (including one anonymous reviewer) for their thoughtful, and constructive feedback.

Conflict of interest

The authors declare that the research was conducted in the absence of any commercial or financial relationships that could be construed as a potential conflict of interest.

Publisher's note

All claims expressed in this article are solely those of the authors and do not necessarily represent those of their

affiliated organizations, or those of the publisher, the editors and the reviewers. Any product that may be evaluated in this article, or claim that may be made by its manufacturer, is not guaranteed or endorsed by the publisher.

Supplementary material

The Supplementary Material for this article can be found online at: https://www.frontiersin.org/articles/10.3389/fmars.2022.934391/full#supplementary-material

References

Barlow, R., Stuart, V., Lutz, V., Sessions, H., Sathyendranath, S., Platt, T., et al. (2007). Seasonal pigment patterns of surface phytoplankton in the subtropical southern hemisphere. *Deep Sea Res. Part I* 54 (10), 1687–1703. doi: 10.1016/j.dsr.2007.06.010

Behrenfeld, M. J., and Kolber, Z. S. (1999). Widespread iron limitation of phytoplankton in the south pacific ocean. *Science* 283 (5403), 840–843. doi: 10.1126/science.283.5403.840

Behrenfeld, M. J., and Milligan, A. J. (2013). Photophysiological expressions of iron stress in phytoplankton. *Annu. Rev. Mar. Sci.* 5, 217–246. doi: 10.1146/annurev-marine-121211-172356

Behrenfeld, M. J., Worthington, K., Sherrell, R. M., Chavez, F. P., Strutton, P., McPhaden, M., et al. (2006). Controls on tropical pacific ocean productivity revealed through nutrient stress diagnostics. *Nature* 442 (7106), 1025–1028. doi: 10.1038/nature05083

Bibby, T. S., Mary, I., Nield, J., Partensky, F., and Barber, J. (2003). Low-light-adapted prochlorococcus species possess specific antennae for each photosystem. *Nature* 424, 1051–1054. doi: 10.1038/nature01933

Browning, T. J., Achterberg, E. P., Rapp, I., Engel, A., Bertrand, E. M., Tagliabue, A., and Moore, C. M. (2017). Nutrient co-limitation at the boundary of an oceanic gyre. *Nature* 551 (7679), 242–246. doi: 10.1038/nature24063

Browning, T. J., Bouman, H. A., Moore, C. M., Schlosser, C., Tarran, G. A., Woodward, E. M. S., et al. (2014). Nutrient regimes control phytoplankton ecophysiology in the south Atlantic. *Biogeosciences* 11, 463–479. doi: 10.5194/bg-11-463-2014

Campbell, D., Hurry, V., Clarke, A. K., Gustafsson, P., and Öquist, G. (1998). Chlorophyll fluorescence analysis of cyanobacterial photosynthesis and acclimation. *Microbiol. Mol. Biol. Rev.* 62 (3), 667–683. doi: 10.1128/MMBR.62.3.667-683.1998

Cullen, J. J., and Davis, R. F. (2003). The blank can make a big difference in oceanographic measurements. *Limnology Oceanography Bull.* 12, 29–35. doi: 10.1002/lob.200312229

Doblin, M. A., Petrou, K. L., Shelly, K., Westwood, K., van den Enden, R., Wright, S., et al. (2011). Diel variation of chlorophyll-a fluorescence, phytoplankton pigments and productivity in the Sub-Antarctic and polar front zones south of Tasmania, Australia. *Deep Sea Res. Part II* 58, 2189–2199. doi: 10.1016/j.dsr2.2011.05.021

Falkowski, P. G., Barber, R. T., and Smetacek, V. V. (1998). Biogeochemical controls and feedbacks on ocean primary production. *Science* 281 (5374), 200–207. doi: 10.1126/science.281.5374.200

Falkowski, P. G., and Raven, J. A. (2007). Aquatic photosynthesis. 2nd edn. Princeton: Princeton University Press

Field, C. B., Behrenfeld, M. J., Randerson, J. T., and Falkowski, P. (1998). Primary production of the biosphere: Integrating terrestrial and oceanic components. *Science* 281 (5374), 237–240. doi: 10.1126/science.281.5374.237

Furuya, K., Hayashi, M., Yabushita, Y., and Ishikawa, A. (2003). Phytoplankton dynamics in the East China Sea in spring and summer as revealed by HPLC-derived pigment signatures. *Deep Sea Res. Part II* 50 (2), 367–387. doi: 10.1016/S0967-0645(02)00460-5

Ho, T. Y., Pan, X., Yang, H. H., George., T. F. W., and Shiah, F. K. (2015). Controls on temporal and spatial variations of phytoplankton pigment distribution in the northern south China Sea. *Deep Sea Res. Part II* 117, 65–85. doi: 10.1016/j.dsr2.2015.05.015

Hsu, M. K., Liu, A. K., and Liu, C. (2000). A study of internal waves in the China seas and yellow Sea using SAR. *Cont. Shelf Res.* 20 (4-5), 389–410. doi: 10.1016/S0278-4343(99)00078-3

Huang, B. Q., Hu, J., Xu, H. Z., Cao, Z. R., and Wang, D. X. (2010). Phytoplankton community at warm eddies in the northern south China Sea in winter 2003/2004. *Deep Sea Res. Part II* 57, 1792–1798. doi: 10.1016/j.dsr2.2010.04.005

Hughes, D. J., Campbell, D. A., Doblin, M. A., Kromkamp, J. C., Lawrenz, E., Moore, C. M., et al. (2018). Roadmaps and detours: Active chlorophyll-a assessments of primary productivity across marine and freshwater systems. *Environ. Sci. Technol.* 52 (21), 12039–12054. doi: 10.1021/acs.est.8b03488

Jiao, N., Zhang, Y., Zhou, K., Li, Q., Dai, M., Liu, J., et al. (2014). Revisiting the CO2 "sourcce" problem in upwelling areas – a comparative study on eddy upwellings in the south China Sea. *Biogeosciences* 11 (9), 2465–2475. doi: 10.5194/bg-11-2465-2014

Jin, P., Gao, G., Liu, X., Li, F., Tong, S., Ding, J., et al. (2016). Contrasting photophysiological characteristics of phytoplankton assemblages in the northern south China Sea. *PloS One* 11 (5), e0153555. doi: 10.1371/journal.pone.0153555

Kolber, Z. S., and Falkowski, P. G. (1993). Use of active fluorescence to estimate phytoplankton photosynthesis *in-situ*. *Limnol. Oceanogr.* 38 (8), 1646–1665. doi: 10.4319/lo.1993.38.8.1646

Kolber, Z. S., Prasil, O., and Falkowski, P. G. (1998). Measurements of variable chlorophyll fluorescence using fast repetition rate techniques: Defining methodology and experimental protocols. *Biochim. Biophys. Acta Bioenerget.* 1367, 88–106. doi: 10.1016/s0005-2728(98)00135-2

Latasa, M. (2007). Improving estimations of phytoplankton class abundances using CHEMTAX. *Mar. Ecol. Prog. Ser.* 329, 13–21. doi: 10.3354/meps329013

Liao, J., Xu, J., Li, R., and Shi, Z. (2021). Photosynthesis-irradiance response in the eddy dipole in the Western south China Sea. *J. Geophys. Res. Oceans* 126 (5), e2020JC016986. doi: 10.1029/2020jc016986

Liu, C. T., Pinkel, R., Klymak, J., Hsu, M. K., Chen, H. W., and Villanoy, C. (2006). Nonlinear internal waves from the Luzon strait. *Eos* 87 (42), 449–451. doi: 10.1029/2006eo420002

Li, H., Wiesner, M. G., Chen, J., Ling, Z., Zhang, J., and Ran, L. (2017). Long-term variation of mesopelagic biogenic flux in the central south China Sea: Impact of monsoonal seasonality and mesoscale eddy. *Deep Sea Res. Part I* 126, 62–72. doi: 10.1016/j.dsr.2017.05.012

Longhurst, A., Sathyendranath, S., Platt, T., and Caverhill, C. (1995). An estimate of global primary production in the ocean from satellite radiometer data. *J. Plankton Res.* 17 (6), 1245–1271. doi: 10.1093/plankt/17.6.1245

Mackey, M. D., Mackey, D. J., Higgins, H. W., and Wright, S. W. (1996). CHEMTAX – a program for estimating class abundances from chemical markers: Application to HPLC measurements of phytoplankton. *Mar. Ecol. Prog. Ser.* 144 (1-3), 265–283. doi: 10.3354/meps144265

Mackey, K. R. M., Paytan, A., Grossman, A. R., and Bailey, S. (2008). A photosynthetic strategy for coping in a high-light, low-nutrient environment. *Limnol. Oceanogr.* 53 (3), 900–913. doi: 10.4319/lo.2008.53.3.0900

Mai, G., Song, X., Xia, X., Ma, Z., Tan, Y., and Li, G. (2021). Photosynthetic characteristics of smaller and larger cell size-fractioned phytoplankton assemblies in the daya bay, northern south China Sea. *Microorganisms* 10(1), 16. doi: 10.3390/microorganisms10010016

McGillicuddy, D. J. (2016). Mechanisms of physical-Biological-Biogeochemical interaction at the oceanic mesoscale. *Annu. Rev. Mar. Sci.* 8 (1), 125–159. doi: 10.1146/annurev-marine-010814-015606

Moore, C. M., Mills, M. M., Arrigo, K. R., Berman-Frank, I., Bopp, L., Boyd, P. W., et al. (2013). Processes and patterns of oceanic nutrient limitation. *Nat. Geosci.* 6, 701–710. doi: 10.1038/ngeo1765

Moore, C. M., Mills, M. M., Langlois, R., Milne, A., Achterberg, E. P., and La Roche, J. (2008). Relative influence of nitrogen and phosphorous availability on phytoplankton physiology and productivity in the oligotrophic sub-tropical north Atlantic ocean. *Limnol. Oceanogr.* 53, 291–305. doi: 10.4319/lo.2008.53.1.0291

Ning, X., Chai, F., Xue, H., Cai, Y., Liu, C., and Shi, J. (2004). Physical-biological oceanographic coupling influencing phytoplankton and primary production in the south China Sea. *J. Geophys. Res. Oceans* 109, C10005. doi: 10.1029/2004jc002365

Pan, X. J., Wong, G. T. F., Shiah, F. K., and Ho, T. Y. (2012). Enhancement of biological productivity by internal waves: observations in the summertime in the northern south China Sea. *J. Oceanogr.* 68 (3), 427–437. doi: 10.1007/s10872-012-0107-y

Raateoja, M., Seppälä, J., and Ylöstalo, P. (2004). Fast repetition rate fluorometry is not applicable to studies of filamentous cyanobacteria from the Baltic Sea. *Limnology Oceanography* 4(4), 1006–1012. doi: 10.4319/lo.2004.49.4.1006

R Development Core Team (2016). *R: a language and environment for statistical computing* (Vienna, Austria: R Foundation for Statistical Computing). Available at: http://cran.R-project.Org.

Schlitzer, R. (2019) *Data analysis and visualization with ocean data view*. Available at: https://odv.awi.de.

Schrader, P. S., Milligan, A. J., and Behrenfeld, M. J. (2011). Surplus photosynthetic antennae complexes underlie diagnostics of iron limitation in a cyanobacterium. *PloS One* 6 (4), e18753. doi: 10.1371/journal.pone.0018753

Schuback, N., and Tortell, P. D. (2019). Diurnal regulation of photosynthetic light absorption, electron transport and carbon fixation in two contrasting oceanic environments. *Biogeosciences* 16 (7), 1381–1399. doi: 10.5194/bg-16-1381-2019

Six, C., Finkel, Z. V., Irwin, A. J., and Campbell, D. A. (2007). Light variability illuminates niche-partitioning among marine picocyanobacteria. *PloS One* 2, e1341. doi: 10.1371/journal.pone.0001341

Suggett, D. J., Moore, C. M., Hickman, A. E., and Geider, R. J. (2009). Interpretation of fast repetition rate (FRR) fluorescence: Signatures of phytoplankton community structure versus physiological state. *Mar. Ecol. Prog. Ser.* 376, 1–19. doi: 10.3354/meps07830

Ting, C. S., Rocap, G., King, J., and Chisholm, S. W. (2002). Cyanobacterial photosynthesis in the oceans: The origins and significance of divergent light-harvesting strategies. *Trends Microbiol.* 10, 134–142. doi: 10.1016/S0966-842X(02)02319-3

Wang, L., Huang, B. Q., Chiang, K. P., Liu, X., Chen, B. Z., Xie, Y. Y., et al. (2016). Physical-biological coupling in the Western south China Sea: The response of phytoplankton community to a mesoscale cyclonic eddy. *PloS One* 11 (4), e0153735. doi: 10.1371/journal.pone.0153735

Wang, L., Huang, B. Q., Laws, E. A., Zhou, K. B., Liu, X., Xie, Y. Y., et al. (2018). Anticyclonic eddy edge effects on phytoplankton communities and particle export in the northern south China Sea. *J. Geophys. Res. Oceans* 123, 7632–7650. doi: 10.1029/2017jc013623

Wang, L., Huang, B., Liu, X., and Xiao, W. (2015). The modification and optimizing of the CHEMTAX running in the south China Sea. *Acta Oceanol. Sin.* 34, 124–131. doi: 10.1007/s13131-015-0621-z

Wei, Y., Chen, Z., Guo, C., Zhong, Q., Wu, C., and Sun, J. (2020). Physiological and ecological responses of photosynthetic processes to oceanic properties and phytoplankton communities in the oligotrophic Western pacific ocean. *Front. Microbiol.* 11, 1774. doi: 10.3389/fmicb.2020.01774

Wen, Z., Browning, T. J., Cai, Y., Dai, R., Zhang, R., Du, C., et al. (2022). Nutrient regulation of biological nitrogen fixation across the tropical western north pacific. *Sci. Adv.* 8, eabl7564. doi: 10.1126/sciadv.abl7564

Wu, J., Chung, S.-W., Wen, L.-S., Liu, K.-K., Chen, Y.-L. L., Chen, H.-Y., et al. (2003). Dissolved inorganic phosphorus, dissolved iron, and *Trichodesmiumin* the oligotrophic south China Sea. *Global Biogeochem. Cycles* 17, 8-1–8-10. doi: 10.1029/2002gb001924

Xiao, W., Wang, L., Laws, E., Xie, Y., Chen, J., Liu, X., et al. (2018). Realized niches explain spatial gradients in seasonal abundance of phytoplankton groups in the south China Sea. *Prog. Oceanogr.* 162, 223–239. doi: 10.1016/j.pocean.2018.03.008

Xie, Y., Laws, E. A., Yang, L., and Huang, B. (2018). Diel patterns of variable fluorescence and carbon fixation of picocyanobacteria prochlorococcus-dominated phytoplankton in the south China Sea basin. *Front. Microbiol.* 9. doi: 10.3389/fmicb.2018.01589

Xiu, P., and Chai, F. (2011). Modeled biogeochemical responses to mesoscale eddies in the south China Sea. *J. Geophys. Res.* 116 (C10). doi: 10.1029/2010JC006800

Xiu, P., Chai, F., Shi, L., Xue, H., and Chao, Y. (2010). A census of eddy activities in the south China Sea during 1993–2007. *J. Geophys. Res.* 115, C03012. doi: 10.1029/2009jc005657

Xu, G., Liu, J., Song, X., Tan, M., Ren, H., Li, D., et al. (2020). Diel rhythm in photosynthetic performance of phytoplankton assemblages is predicted to be light-dependent from *in situ* and mesocosm chlorophyll fluorescence. *J. Coast. Res.* 104 (SI), 445–454. doi: 10.2112/JCR-SI104-080.1

Zhang, M., Wu, Y., Wang, F., Xu, D., Liu, S., and Zhou, M. (2020). Hotspot of organic carbon export driven by mesoscale eddies in the slope region of the northern south China Sea. *Front. Mar. Sci.* 7. doi: 10.3389/fmars.2020.00444

Zhao, Z. X., Klemas, V., Zheng, Q. N., and Yan, X. H. (2004). Remote sensing evidence for baroclinic tide origin of internal solitary waves in the northeastern south China Sea. *Geophys. Res. Lett.* 31 (6), L06302. doi: 10.1029/2003gl019077

Zhu, Y., Feng, Y., Browning, T. J., Wen, Z., Hughes, D. J., Hao, Q., et al. (2022). Exploring variability of trichodesmium photophysiology using multi-excitation wavelength fast repetition rate fluorometry. *Front. Microbiol.* 13, 813573. doi: 10.3389/fmicb.2022.813573